A THEORY OF NECROTAXIS

CHIA-LUN H U and FRANK S. BARNES

From the Department of Electrical Engineering, University of Colorado, Boulder, Colorado 80301

ABSTRACT A mathematical theory for the motion of polynuclear leukocytes after the laser irradiation of a red blood cell is derived and compared with the measured movement of a number of cells. An estimate is made on the diffusion constant and the molecular size for the unknown material which communicates the information on the irradiation of the red blood cell to the leukocyte.

INTRODUCTION

Necrotaxis is a special kind of chemotaxis. When a red or white blood cell is selectively killed by laser irradiation, the surrounding polynuclear leukocytes, which make up a fraction of the white blood cells, will sense the death of this cell and start moving toward it. The leukocytes reaching the dead cell eat the corpse. The velocity distribution of a typical leukocyte is shown in Fig. 1. This velocity first increases, stays constant for a while, then decreases to zero. It is the purpose of this paper to propose a mathematical theory for the motion of the leukocytes and to obtain an estimate of the diffusion coefficient of the unknown substance which notifies the white cells that the cell has been irradiated.

Chemotaxis was discovered as early as the 19th century when people observed the movement of spermatozoids towards the ovaries of certain cryptogams (1). Several similar phenomena have been then observed experimentally by Leber (2), Comandon (3), McCutcheon et al. (4), and Harris (5–7). Particularly for necrotaxis, Harris (5–7), Bessis (8, 9), and Thompson (10) have done extensive experimental work in recent years. As it has been suggested by Bessis and Burte (9) the attracting force acting on the attacking white cells is due to the concentration gradient of certain "active" materials diffusing from the broken cell. However, to our knowledge, there is no theory which explains (*a*) how the driving force depends on the concentration gradient; and (*b*) what material diffusing from the dead cell is responsible for the motion of the leukocytes. The analytical work reported in this article yields a method of deriving the driving function for the leukocytes in terms of a concentration gradient which is consistent with the measured leukocyte velocity curves and the expected distribution of the unknown chemical in time and space.

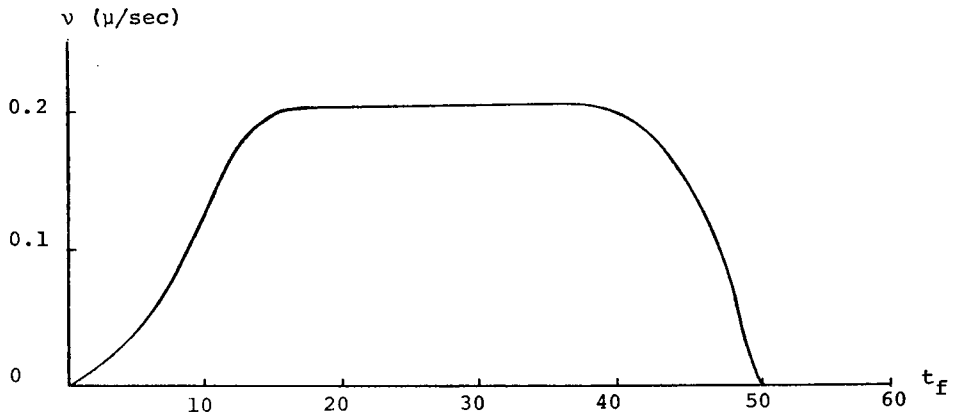

FIGURE 1 Velocity distribution of a typical leukocyte.

FORMULATING THE PROBLEM

In order to simplify the analysis, we are forced to make several assumptions, namely,

(*a*) The cells are considered as particles, instead of three dimensional objects. This is a good assumption if the initial separation between the cells is large enough to compare with the dimensions of the cells, and if the internal structure of polynuclear leukocytes is neglected. Detailed observations of these cells show that there is an oriented internal structure which affects the delay time between the laser irradiation of the red blood cell and the onset of motion by the white cell, however, our treatment will neglect this structure and its influence on white cell motions.

(*b*) The only resistance force acting on the white cells is due to viscosity of the body fluid.

(*c*) Only a two-cell system is considered here. Therefore the diffusion of the active material is not perturbed by the presence of other cells. In the experiments we observed that there are a significant number of cases where the white cells travel winding paths instead of straight ones toward the center of the dead cell. These winding paths can often be explained by the fact that the diffusion of the active material has been disturbed by the presence of other white cells or other impervious material. Consequently the direction of the driving force (which is parallel to ∇C)[1] does not always point to the center of the dead cell as it would if there were no perturbation of the diffusion pattern. However, in the analysis, we have selected 25 sets out of 125 sets of raw experimental data as the unperturbed

[1] If one accepts the primary assumption that the attracting message which drives the white cells to move is similar to the smell of a fox which drives the hunting dogs to pursue, then, the direction of the driving force must be along the direction of ∇C. However, the magnitude of the driving force may be a very particular increasing function of $|\nabla C|$. To determine this function is one part of the goal of this paper.

ones for analysis. These selected data show approximately straight-line centripetal displacements for the motion of the white cells. Therefore, as far as these selected data are concerned, assumption *c* should be a good one.

With these assumptions, one can formulate the motion equation of a typical white cell as follows:

$$m\frac{d^2|r|}{dt^2} + \sigma\frac{d|r|}{dt} = -f[|\nabla c(r, t)|]. \tag{1}$$

Boundary conditions

$$\begin{cases} r = r_0 \text{ at } t = 0 & (2) \\ r = 0 \text{ permanently after } t \geq t_f\,, & (3) \end{cases}$$

where m is the mass of the white cell, $\sigma = 6\pi\eta a$ is the Stoke coefficient, r is the radial distance of the white cell from the dead cell, and f is the driving function. The first term is the term for the inertial force, the second, the viscosity force, and the third, the driving force. We use the absolute value of r here because by the symmetry of a two particle system. Whether the moving particle is approaching, $(+ r)$ or leaving $(- r)$ the attracting particle, the absolute value of r should satisfy the same equation of motion.[2] We will see later that this absolute value of r is responsible for the second boundary condition. The function f is to be determined by comparing the theory with the experiments.

Before attempting to solve this equation, it is worthwhile to compare the size of the first two terms. Experimental plots of r as a function of time show only slow changes with time. The order of $d^2|r|/dt^2$ and $d|r|/dt$ should be approximately the same as those of r_0/t_f^2 and r_0/t_f, respectively where r_0 is the initial separation between the laser cell and the white cell, t_f is the final time for the white cell to reach the center of the dead cell. For a typical set of the experimental data: $r_0 = 0.01$ cm; $t_f = 100$ sec; a = average linear dimension of the white cell = 10^{-3} cm; η = viscosity of the body fluid = 0.01 poise; m = the mass of the white cell $\simeq \rho_{H_2O} \cdot a^3 = 10^{-9}$ g, $\sigma = 6\pi \times 10^{-3} \times 10^{-2} = 10^{-4}$ cgs. The first term is approximately 10^{-15} and the second term $\approx 10^{-8}$. Therefore the first term can be neglected in comparison to the second term and the motion equation is simplified to:

$$\frac{d|r|}{dt} = \frac{-1}{\sigma} f(|\nabla C|). \tag{4}$$

To calculate ∇C in the driving term, we assume that C is the concentration of the material diffusing from a line source released at $t = 0$. This line source is sand-

[2] If the driving term f has a factor, say $r^{0.5}$, then, without the absolute value for r, this equation would have no meaning when r is negative because $r^{0.5}$ is imaginary. On the other hand, if f contains a factor $|r|^{0.5}$ but on the left hand side of the equation there is no absolute value for r, then, the two branches of the equation for $r < 0$ and $r > 0$ will not be in symmetrical form. Consequently, we need an absolute value of r throughout the whole equation.

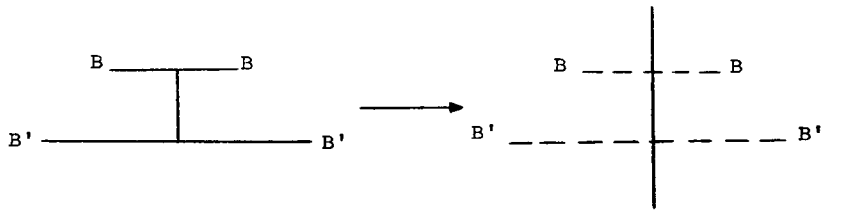

FIGURE 2 Line source between two perpendicular nonpermeable walls.

wiched between two perpendicular nonpermeable walls as shown in Fig. 2. This diffusion model resembles the case of the dead cell which is sandwiched between the microscope slide and cover slip used in the experiments. Mathematically this line source is equivalent to removing the boundary walls and extending the line source to infinity. This condition is known as the Neumann's boundary conditions and the concentration function is just the two dimensional Green function for the diffusion equation:[3]

$$C(r, t) = \frac{\lambda}{4\pi Dt} e^{-r^2/4Dt}, \tag{5}$$

where λ is the initial mass per unit length of the unreleased source, D is the diffusion coefficient. Calculating $|\nabla C|$ yields:

$$|\nabla C| = \left|\frac{\partial C}{\partial r}\right| = \frac{\lambda |r|}{8\pi D^2 t^2} e^{-r^2/4Dt}. \tag{6}$$

If we substitute equation 6 into equation 4 with the boundary conditions of equations 2 and 3, we obtain

$$\frac{d|r|}{dt} = -\frac{1}{\sigma} f\left[\frac{2\lambda}{\pi} \frac{|r|}{(4Dt)^2} e^{-r^2/4Dt}\right] \tag{7}$$

$$r = r_0 \text{ at } t = 0 \tag{8}$$

$$r = 0 \text{ permanently at } t > t_f . \tag{9}$$

In order to solve equation 7, we have to determine the function f. Equation 7 is a first-order ordinary differential equation with two boundary conditions, equations 8 and 9. Therefore function f cannot be chosen arbitrarily. In fact, if we assume $f(x)$ can be expanded in the form[4]

$$f(x) = x^n(a_0 + a_1 x + a_2 x^2 + \cdots). \tag{10}$$

---

[3] P. M. Morse and H. Feshback. *Method of Theoretical Physics*. McGraw-Hill Book Company, New York. 880.

[4] If we directly expand $f(x)$ in an ascending power series, then the zeroth order term cannot exist because otherwise $f(0) \neq 0$, or in other words, without concentration gradient there is still a static driving force acting on the white cell. This is physically impossible. Therefore the zeroth order term must vanish or $f(x) = a_1 x + a_2 x^2 + \cdots$. But this is just a special case of equation 10 with $n = 1$.

then as is proved in the Appendix, n must be smaller than 1, or $0 < n < 1$ must hold, when the higher-order terms are neglected. By comparing these theoretical solutions with respect to the experimental results we will be able to determine the power index n of the controlling factor in the function f.

If we consider only the controlling factor and neglect the higher order term in equation 10, then, the right-hand side of equation 7 is always negative. Therefore the *absolute value* of r always *decreases* with respect to time. Consequently $r = 0$ is a stable point in the solution. Consequently equation 9 will be satisfied automatically if the solution of the following equation will have a point that $r = 0$ at $t = t_f$ (some finite time)

$$\frac{dr}{dt} = -\left[\frac{2\lambda}{\pi\sigma'}\frac{r}{(4Dt)^2}e^{-r^2/4Dt}\right]^n, \qquad r \geq 0 \quad (11)$$

$$= -k\left[\frac{r}{t^2}e^{-r^2/4Dt}\right]^n \quad (11)$$

$$r = r_0 \text{ at } t = 0, \quad (12)$$

where $k \equiv [\lambda/(8\pi\sigma' D^2)]^n$ and $\sigma' \equiv \sigma^{1/n}$. In the Appendix, it is shown that there *is* such a point in the solution *only* when n lies between 0 and 1.

The problem is now reduced to solving equation 11 with a single boundary condition, equation 12.

SOLVING THE PROBLEM

Equation 11 is a nonlinear differential equation with no apparent integrating factor. It can be solved by numerical analysis. However, applying numerical analysis to equation 11 directly is difficult because it contains two unknown coefficients, namely k and D.

If we introduce the normalized quantities R, T such that $r = \alpha R$, $t = \beta T$, into equations 11 and 12, then we can adjust the normalization factors α, β to obtain the following equations:

$$\frac{dR}{dT} = -\left[\frac{R}{T^2}e^{-R^2/T}\right]^n$$

$$R = 1 \text{ at } T = 0. \quad (13)$$

The adjustment we need to make on α and β is such that the following conditions must hold.

$$\frac{\alpha^2}{4D\beta} = 1, \qquad \frac{\alpha^{n-1}}{\beta^{2n-1}} = \frac{1}{k} \quad (14)$$

$\alpha = r_0$ (from the boundary condition) $\qquad \beta = \frac{t_f}{T_f}$ (from the definition $t = \beta T$)

where T_f is the root of $R(T_f) = 0$ and $R(T)$ is the solution of equation 13. There are four unknowns, α, β, D, and k, in the four parts of equation 14. r_0 and t_f are experimentally known data. Solving D and k explicitly from equation 14, we have

$$D = \frac{1}{4}\frac{r_0^2 T_f}{t_f}$$

$$k = (t_f/T_f)^{2^{n-1}}/r_0^{n-1}. \tag{15}$$

Returning to equation 13, we see that the motion equation and the boundary condition are completely free of unknown coefficients now. Therefore numerical method may be applied. We used Euler's method to solve this nonlinear equation and the resultant velocity curves for various n's are plotted in Fig. 3. It is seen that when the index n goes higher and higher, the velocity curve will be steeper and steeper. When n approaches zero, the velocity curve will approach the flat-top rectangular distribution as shown in Fig. 3. The reason for this can be easily seen in the following.

If n is a very small number, then,

$$\lim_{n \to 0} (a^n) = 1, \text{ when } a > 0$$

$$\lim_{n \to 0} (a^n) = 0, \text{ when } a = 0. \tag{16}$$

Now let the bracket of the right-hand side of equation 13 be called as $g(R, T)$

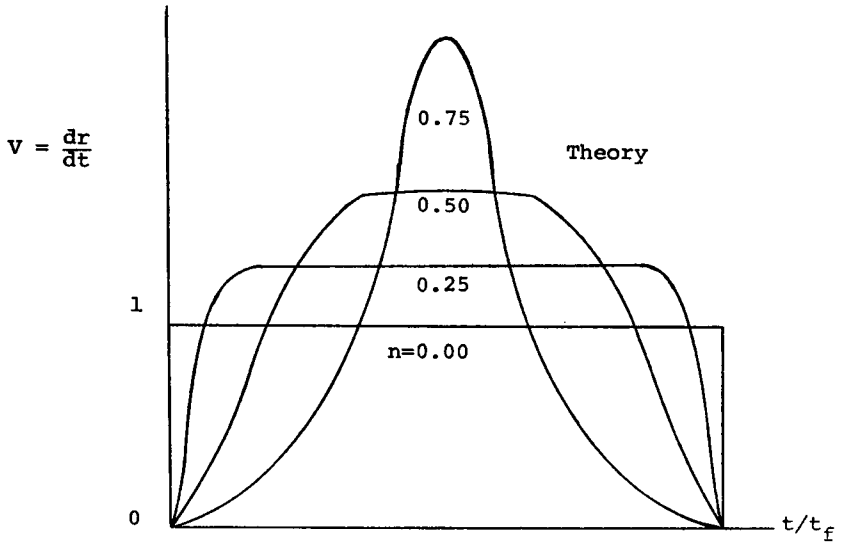

FIGURE 3 Velocity curves for various n's, using Euler's method to solve equation 13.

then $g(R, T)$ has the following properties:

$$g(R, T) = \frac{R}{T^2} e^{-(R^2/T)} \begin{cases} = 0 & T = 0, R \neq 0 \text{ or} \\ & T \neq 0, R = 0 \\ > 0 & \text{otherwise.} \end{cases} \quad (17)$$

$g(R, 0) = 0$ can be verified by applying L'Hospital's rule.

Combining equations 16 and 17, we see immediately that the velocity curve for $n = 0$ is

$$V_{n=0}(R, T) = \lim_{n \to 0} g^n = \begin{cases} 0, & T = 0, R \neq 10 \text{ or} \\ & T \neq 0, R = 0 \\ 1, & \text{otherwise,} \end{cases} \quad (18)$$

i.e., when $n = 0$, the velocity curve is a rectangular pulse as shown in Fig. 3.

If we plot the normalized experimental points as shown in Fig. 4 and compare them with the theoretical curves, we see that the best fit theoretical curve will be that corresponding to $n = 0.25$ which is redrawn in Fig. 4. Thus the driving force acting on the white cell appears to be approximately proportional to the 0.25 or ¼ power of the concentration gradient of the active material diffusing from the dead cell.

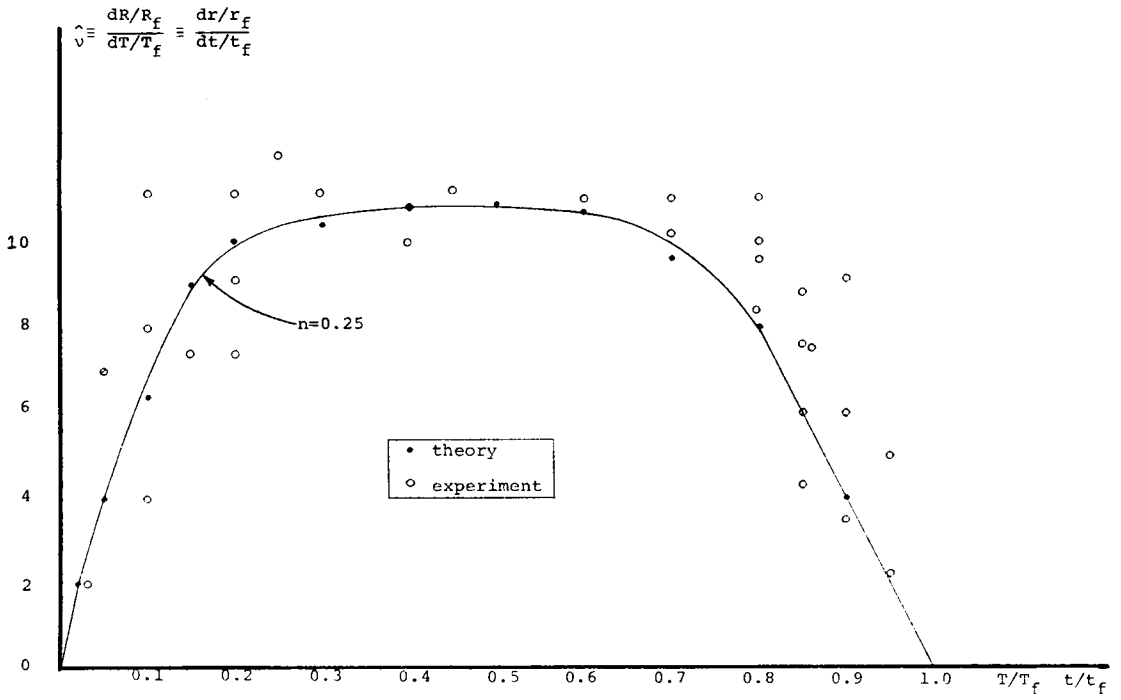

FIGURE 4 Normalized experimental points.

The measurements for Fig. 4 were made from a video tape replay of the motions of the white cells as observed through a phase contrast microscope on a Sony TV camera system. The magnification of the system is approximately 1000. This system allowed us to observe the cell motions in real time and then conveniently replay the tapes for making coordinate measurements relative to laser-irradiated red blood cells as a function of time. The ruby laser, microscope, and camera system are all described in more detail by Bessis et al. in references 11 and 12.

The blood was obtained from donors in good health. 10 ml of blood were mixed with 0.2 ml of Calciparine Choay ($\frac{1}{20}$). Sedimentation occurred at laboratory temperature and polynuclear white cells were obtained after about $1\frac{1}{2}$ hr. Monocytes and lymphocytes were contained in larger fractions in samples after $\frac{1}{2}$ hr and while the cells were suspended in the plasma.

Studies of the effect of parameter variations have been initiated. Preliminary modifications were that a reduction in velocity occurs with a drop in the temperature of the plasma, and the degree of coagulation. This is to be expected as the result of an increase in the viscosity of the material. The measured range of velocities varied from 0.13 μ/sec to 0.65 μ/sec. The spread in the mean velocities from cell to cell under the same operating conditions was as much as 40% and ranged from ± 0.8 μ/sec to ± 0.14 μ/sec. These variations may result from unequal irradiations of various parts of red blood cell and to inhomogeneities in the blood plasma. The maximum distance from the target red cell to the migrating white cell increases with increasing laser energy. The same velocity profiles were obtained from laser-irradiated cells from which most of the hemoglobin has been removed. This evidence along with that from references 13 and 14 leads us to postulate that the chemical which communicates with the leukocytes is generated by heating the cell membrane in the presence of the plasma. Experiments are now in progress to check this hypothesis. The second part of the goal of this work is to identify the active material responsible for the dragging action. This can be done by determining the diffusion coefficient first and then calculating the molecular weight of this material from this diffusion coefficient.

From the numerical solution corresponding to $n = \frac{1}{4}$, we obtain that $T_f = 1.49$ at $R = 0$. Substituting this T_f and the experimental values of r_0 and t_f into equation 15, we obtain that

$$D \approx 10^{-7}, \text{ cm}^2/\text{sec}$$

$$k \approx 4 \times 10^{-3} \text{ (cm)}^{3/4}/\text{(sec)}^{1/2}.$$

It should be pointed out here that the variation of D is quite large (about 50%$\pm$) because of the scattering of the experimental points. However, with the above value of D, we can estimate the order of the molecular weight of the active material.

There is a well known formula in statistical physics that connecting the diffusion

coefficient with the molecular weight of the diffusion particle if one knows the density of this particle. This formula is

$$M = \left(\frac{RT}{6\pi\eta ND}\right)^3 \frac{\rho}{m_p},$$

where R = gas constant = 8.3×10^7 cgs; T = absolute temperature = 300 K; η = viscosity coefficient of the fluid (for body fluid, $\eta = 10^{-2}$ poise); N = Avogadro constant = 6×10^{23} number of molecules/mole; m_p = mass of proton = 1.7×10^{-24} g; and ρ = density of the active molecule $\approx \rho(H_2O) = 1$ g/cm^3.

If one substitutes the value of D into this formula, then one has $M = 10{,}000$. However, since M depends on the inverse cubic power of D and D has not been accurately determined as just mentioned, we can only say that the molecular weight of the active material has an order of 10,000's. It should be noted that this estimated molecular size is probably large because we are characterizing the motion of the leukocyte as a function of a single input parameter. In fact, its motion is probably the result of several complex chemical reactions; the first of which is activated by our communicating substance and each of which take some time to occur.

In order to obtain better values of D and thus M, a number of experiments are in progress.

APPENDIX

Theorem

If the equation of motion of a leukocyte takes the form of $dr/dt = -[B \mid \nabla C \mid]^n$ *then, n must be less than* 1.

The boundary condition which leads to this restriction is that of equation 3 in the text. To prove this theorem, we have to divide the proof into three parts. First to prove that for $n = 1$ and $n > 1$, equation 3 can never be satisfied, then, in the third part, it is proved that for $n < 1$, equation 3 cancertainly be satisfied.

Lemma 1 *When* $n = 1$, *equation* 3 *can never be satisfied.*

Proof. If one makes a transformation of the variables that $t = 1/\alpha x$, $r_1 = \beta y$ to the equation (subscript 1 here means that $n = 1$):

$$\frac{dr_1}{dt} = -\frac{2\lambda B}{\pi\sigma} \frac{r_1}{(4Dt)^2} e^{-r_1^2/4Dt}, \tag{A 1}$$

then, one can adjust α, β to obtain the following equation

$$\frac{dy}{dx} = ye^{-xy}. \tag{A 2}$$

Now, if $r = 0$ occurs at some finite $t = t_f$ as required in the condition of equation 3, then, $y = 0$ must necessarily occur at some $x = x_f$. Thus from equation A 2, one can see that $y' = dy/dx = 0$ at $x = x_f$. Moreover, differentiating equation A 2 with respect to x, and

keeping in mind that y is a function of x, one has then,

$$y'' = [y' - y(y + xy')]e^{-xy}.$$

This vanishes again at $x = x_f$, because $y = 0$ and $y' = 0$ at $x = x_f$.

Following the same procedures, one soon discovers that for any order derivative of y, every term in the right-hand side must contain either the lower derivatives of y or y itself. Therefore all derivatives of y must vanish at $x = x_f$. Consequently, $y = 0$ necessarily for all x. Because by Taylor's expansion of y at $x = x_f$, the coefficient of every term of the series vanishes. This means that if equation 3 is to be satisfied, the only solution is $r \equiv 0$ (identically for all t). This completes the proof of this lemma.

An immediate result of this lemma is that when $n = 1$ and if r_{10} (the initial value of r_1) $\neq 0$, r_1 can never reach zero at any t. r_1 vanishes at a certain t only when $r_1 = 0$ identically, i.e., the graphs of $r_0(t)$ when r_{10} is varied look like that shown in Fig. 5.

It is to be noted also that for any point in the $r_1 - t$ plane, there is one and only one curve passing through this point, because, by equation A 1, there is only one definite slope at any given point (r_1, t).

Lemma 2 *If $n > 1$, equation 3 can never be satisfied.*

Proof. If $dr_n/dt = -(B \mid \nabla C \mid)^n$, $n > 1$, then r_n is a continuously decreasing function of t whenever $r_n > 0$, because the right-hand side of the above equation is always negative. If one assumes that $r_n = 0$ at some t, then this lemma is proved if one can prove that a contradiction (r_n cannot be equal to zero) must arise.

If $r_n = 0$ at some t, then, there certainly exists some r_a and t_a such that

$$\frac{2\lambda B}{\pi\sigma} \frac{r_a}{(4Dt_a)^2} < 1 \text{ whenever } t > t_a. \qquad (A\ 3)$$

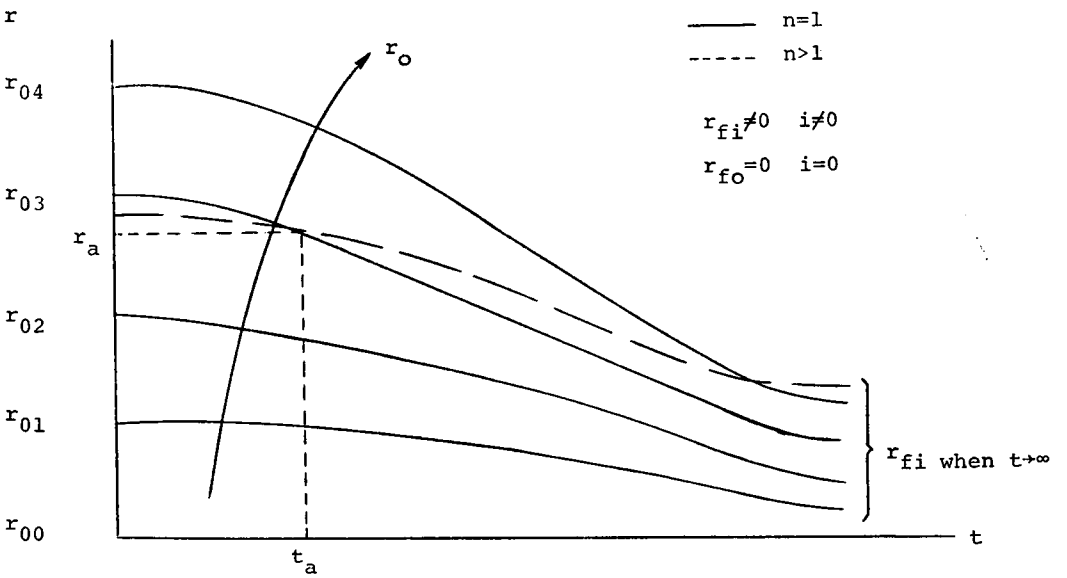

FIGURE 5 Graphs of $r_1 t$ when r_{10} is varied.

At this (r_a, t_a) point, there must be a curve of $n = 1$ passing through as shown in Fig. 5. Now, we want to prove that when $t > t_a$, $dr_n/dt > dr_1/dt$ must hold. Therefore the $n > 1$ curve always decreases *slower* than the $n = 1$ curve does after this point (Fig. 5). Consequently, r_n cannot go to zero (a contradiction to what had just been assumed), because $n = 1$ curve cannot go to zero as proved in lemma 1.

It is very easy to see that $dr_n/dt > dr_1/dt$ after (r_a, t_a) point because of equation A 3,

$$\left[\frac{2\lambda B}{\pi\sigma}\,\frac{r}{(4Dt)^2}\right]^n < \frac{2\lambda B}{\pi\sigma}\,\frac{r}{(4Dt)^2} \quad \text{for} \quad t > t_a.$$

Also $[e^{-r^2/4Dt}]^n < e^{-r^2/4Dt}$ should be valid because $e^{-r^2/4Dt} < 1$. By these two inequalities and the equations that

$$\frac{dr_n}{dt} = -A^n, \qquad \frac{dr_1}{dt} = -A,$$

where

$$A \equiv \frac{2\lambda B}{\pi\sigma}\,\frac{r}{(4Dt)^2}\,e^{-r^2/4Dt},$$

it follows immediately that

$$\frac{dr_n}{dt} > \frac{dr_1}{dt} \quad \text{after} \quad t > t_a.$$

This thus completes the proof.

Proof of the Theorem. (If $n < 1$, equation 3 can certainly be satisfied.)

Following the same technique used in the proof of lemma 2, we can see that, for $n < 1$, $dr_n/dt < dr_1/dt$ after a certain cross-over point (r_a, t_a). (A 4)

This shows that after t_a, the $r_n - t$ curve will be *lower* than $r_1 - t$ curve. Now there are three possibilities for the behavior of the $r_n - t$ curve after this cross-over point: (*a*) it will recross over the $r_1 - t$ curve at some further t; (*b*) it will approach zero under the $r_1 - 1$ curve; and (*c*) it will intersect the t-axis, or r_n will be equal to zero, at some finite time t_f. The first two cases must be excluded because they require that $dr_n/dt > dr_1/dt$ after some finite $t_b (t_b > t_a)$ which is not allowed by equation A 4. Therefore the $r_n - t$ curve will intersect the t-axis at some finite time t_f.

After t_f, r_n will still be equal to zero as provided in the text. Therefore equation 3 can be satisfied automatically when $n < 1$.

We wish to express our appreciation to Professor Bessis in whose laboratory the experimental work was done and to Madam Barat and Anne Boisfleury for carrying out the experimental measurements which are summarized in Fig. 4.

We also wish to express our appreciation for financial support by the National Institute of Health' the Office of the Army Surgeon General, and the French Government.

Received for publication 9 October 1969 and in revised form 30 March 1970.

REFERENCES

1. PFEFFER, W. 1884. *Undersuch. Botan. Inst. Zu Tubingen.* 1:363.
2. LEBER, T. 1891. Die Entstehung der Entzyndung. Engelmann, Leipzig.

3. COMANDON, J. 1917. *C. R. Seances Soc. Biol. Filiales.* **80**:314.
4. MCCUTCHEON, M., D. R. COMAN, and H. M. DIXON. 1939. *Arch. Pathol.* **27**:61.
5. HARRIS, H. 1953. *J. Pathol. Bacteriol.* **66**:135.
6. HARRIS, H. 1953. *Brit. J. Exp. Pathol.* **34**:276.
7. HARRIS, H. 1961. Function of the Blood. Academic Press Inc., New York. 463–492.
8. BESSIS, M. 1964. CIBA Foundation Symposium on Cellular Injury. CIBA Foundation, Churchill, London. 287–316.
9. BESSIS, M., and B. BURTE. 1965. *Tex. Rep. Biol. Med.* **23** (Suppl. 1): 204.
10. THOMPSON, P. L., J. M. PAPADIMITIOU, and M. WALTERS. 1967. *J. Pathol. Bacteriol.* **94**:339.
11. BESSIS, M., F. GIRES, G. MAYER, and G. NOMARSKI. 1962. *C. R. Acad. Sci.* **255**:1010.
12. BESSIS, M., and M. TER-POGOSSIAN. 1964. Micropuncture of cells by means of a Laser beam. New York Academy of Science, New York.
13. BESSIS, M., and B. BURTE. 1965. *Tex. Rep. Biol. Med.* **23** (Suppl. 1):204–212.
14. GOWLAND, E. 1964. *J. Pathol. Bacteriol.* **87**: 347.